RESEARCH PAPER

# Mortar Properties Improvement by Using Fine Portland Cement Clinker as Reactive Aggregate

**Jafar Shafaghat[1] and Ali Allahverdi[1,2*]**

** ali.allahverdi@iust.ac.ir*

**Received: September 2018 Revised: March 2019 Accepted: May 2019**

[1] Research Laboratory of Inorganic Chemical Process Technologies, School of Chemical Engineering, Iran University of Science and Technology, Tehran, Iran
[2] Cement Research Center, Iran University of Science and Technology, Tehran, Iran

**DOI: 10.22068/ijmse.18.1.5**

***Abstract:*** *Microscopic studies has shown that adjacent to the interface between cement paste and aggregate, there exists an area with high porosity and low binding compounds that is referred to as interfacial transition zone (ITZ). ITZ in concrete and mortar imposes a number of negative effects, including flexural and compressive strengths reduction and permeability enhancement. That's why many research attempts have been devoted to limit ITZ and its negative effects. The present study investigates the possibility of utilizing fine Portland cement (PC) clinker as a reactive aggregate in mortar for the same purpose. For this, natural quartz sand in normal mortar (NM) was totally replaced with PC clinker of the same particle size distribution and the most important engineering properties of the new mortar referred to as Reactive Aggregate Mortar (RAM) were measured and compared with NM as control. The results of compressive strengths measurements represented 65 and 21% increase after curing age of 7 and 90 days, respectively, for RAM compared to NM. Chloride penetration depth in RAM displayed reductions by about 33 and 26% after 14 and 28 days of exposure, respectively. The effect of PC clinker reactivity on the microstructure and size of ITZ was studied by using scanning electron microscopy.*

***Keywords:*** *Interfacial transition zone, Mortar, Portland cement clinker, Compressive strength, Chloride penetration depth.*

## 1. INTRODUCTION

Microscopic studies on concrete indicate that there exists a region with high porosity and low binding compounds at the interface of cement paste and aggregate, which is referred to as the interfacial transition zone (ITZ) [1]. Although different values have been reported for the thickness of ITZ, it can be claimed that ITZ thickness ranges from 10 to about 60 microns in many concretes [2-4]. The content of portlandite as a non-binding compound is usually high in ITZ and calcium silicate hydrate (C-S-H) gel, which is the most important binding compound in concrete, has a low content in this region [5]. ITZ, therefore, imposes very important negative effects on concrete properties. In summary, it reduces the compressive and flexural strengths as well as durability in aggressive environments [6]. For this reason, many attempts have been devoted to improving the microstructure of the ITZ and limiting its negative effects [7-13]. Nili and Ehsani [7] used nano silica and silica fume to improve the ITZ complex microstructure. It was found that addition of 3% or 5% nano silica significantly increases the compression strength of concrete. They claimed that microstructural analyses by SEM and EDS revealed that this increase was due to modifications in ITZ microstructure brought about by nano silica. Cohen et al.'s experiments [8] showed that the use of silica fume alone is also effective in improving the ITZ microstructure. Metakaolin is another materials that is used to improve the negative effects of the ITZ [9, 10]. Duan et al. [9] observed that incorporation of 10 wt.% of metakaolin effectively refines the pore structure as well as ITZ [9]. Ground granulated Blast furnace slag is another supplementary cementing material that has been used to improve the ITZ properties. Duan et al. [9], however, reported a weaker pore structure refinement effect for ground granulated Blast furnace slag compared to metakaolin and silica fume. Rice husk ash (RHA), as a reactive pozzolanic material, has also been used to improve the microstructure of ITZ. He et al [11] investigated the influence of RHA on hydration products and ITZ microstructure. They reported that incorporation of RHA reduces the ITZ thickness and increases



[ DOI: 10.22068/ijmse.18.1.5 ]

the elastic modulus of the matrix. Chao-Lung et al. [12] reported that replacing cement with RHA is beneficial only up to 20 wt.% and higher replacement levels adversely affects the concrete properties [12]. Givi et al. [13] evaluated the size effect of RHA in concrete properties. They concluded that ultra-fine RHA with an average particle size of 5 micron is more effective in increasing compressive strength and reducing water permeability of concrete compared to normal RHA with an average particle size of 95 micron. Physical properties of aggregate such as size can also considerably affect the size of ITZ and, therefore, the concrete properties. Ping et al [14] studied the effects of aggregate size and type on ITZ properties and concluded that ITZ thickness decreases with the decreasing of the aggregate size, regardless of the aggregate type.

Since portland cement (PC) clinker is a reactive material producing binding compounds on its surface when comes in contact with water, Berger et al. [15] used PC clinker instead of natural aggregate in concrete. Considering a concrete of limiting maximum aggregate size of approximately 9.5 mm and replacing the natural aggregate with PC clinker, they concluded that substitution of natural aggregate with PC clinker results in substantial increases in concrete mechanical properties. In a recent work, Shafaghat et al. [16] replaced aggregate larger than 1 mm with PC clinker of the same size and determined its effect on concrete properties. They reported significant improvements in concrete properties through ITZ microstructure refinement. Since concrete properties depend on aggregate size and most of the published data on ITZ improvement is devoted to portland cement concretes of relatively large aggregate sizes rather than portland cement mortars, this work is devoted to improving ITZ microstructure in portland cement mortar of fine aggregate. In the present work, the natural quartz sand of limiting maximum size of 1 mm in a normal mortar (NM) was completely replaced with a PC clinker of exactly the same particle size distribution as an artificial reactive aggregate to eliminate or effectively reduce ITZ thickness. The fresh and hardened properties of this new reactive aggregate mortar (RAM) were measured and compared to NM. Scanning electron microscopy was also used to investigate the effect of PC clinker as a reactive aggregate on microstructure and dimensions of ITZ.

## 2. EXPERIMENTAL PROCEDURES

### 2.1. Materials and Preparation Methods

Type 2 PC (in accordance with ASTM C150-17 [17]) of strength grade 42.5 and PC clinker of the same PC with a density of 3112 kg/m$^3$ were prepared from Tehran cement company, Tehran, Iran. The main oxide composition and the Bogue's potential quaternary phase composition of the cement and clinker are given in Table 1.

**Table 1.** Main oxide and Bogue's potential phase compositions of cement and clinker.

| Material | Main oxides (wt.%) | | | | Phases (wt.%) | | | |
|---|---|---|---|---|---|---|---|---|
| | CaO | $SiO_2$ | $Al_2O_3$ | $Fe_2O_3$ | $C_3S$ | $C_2S$ | $C_3A$ | $C_4AF$ |
| PC | 62.62 | 21.52 | 4.66 | 3.40 | 50.7 | 33.4 | 6.6 | 10.3 |
| PC clinker | 63.14 | 22.52 | 5.50 | 3.96 | 43.2 | 32.0 | 7.9 | 12.1 |

The maximum particle size for standard sand for mortar is limited to 2 and 1.18 mm in EN 196-1 and ASTM C778, respectively. For this and for practical purposes, a typical commercially available and well-washed natural quartz sand with a density of 1201 kg/m$^3$ and a grain size in the range between 1 to 0.25 mm, used in this research, was prepared from the mines around Amol on the margin of the Haraz River, Mazandaran, Iran. Table 2 represents the particle size distribution of the sand and PC clinker. PC clinker was firstly separated into the same size fractions as quartz sand (see Table 2) and then the same weight fractions were recombined to obtain a very similar size distribution.

**Table 2.** Particle size distribution of quartz sand and Portland cement clinker.

| Size fraction (mm) | wt. % |
|---|---|
| 1 – 0.68 | 37 |
| 0.68 – 0.55 | 20 |
| 0.55 – 0.25 | 43 |

A total number 24 mortar prisms from each NM and RAM were prepared and cured in accordance with ASTM C192-16 [18]. The aggregate-to-cement mass ratio in NM was controlled at 2.75, which was equal to an aggregate-to-cement volume ratio of 2.207. Since PC clinker possessed a different density, the same aggregate-to-cement volume ratio was applied for RAM. A water-to-cement mass ratio of 0.545 that resulted in a flow table between



[ DOI: 10.22068/ijmse.18.1.5 ]

105 to 115 mm in 25 drops of the flow table was applied for both NM and RAM in accordance with ASTM C230-14 [19] and ASTM C1437-15 [20]. After casting, the fresh mortars were kept in humid chamber with a relative humidity more than 95% for the 1 day and then the mortar prisms were cured in water until the experiment time. During the curing period, the temperature was controlled between 23.0 ± 2.0 ˚C. Mix design of NM and RAM are represented in Table 3.

**Table 3.** Mix design of NM and RAM (kg/m$^3$)

| | NM | RAM |
|---|---|---|
| Cement | 450 | 450 |
| Water | 245 | 245 |
| Total aggregate | 1690 | 1514 |
| Sand | (1690) | (0) |
| PC clinker | (0) | (1514) |
| Water-to-Cement mass ratio | 0.545 | 0.545 |
| Aggregate-to-Cement volume ratio | 2.207 | 2.207 |

## 2.2. Testing Methods

### *2.2.1. Workability and Setting Time*

Workability of fresh mortars was determined using a flow table in accordance with ASTM C230-14 [19] and ASTM C1437 [20]. Setting time of the fresh mortars was also measured using a specific Vicat needle in accordance with ASTM C807-13 [21].

### *2.2.2. Compressive and Flexural Strengths*

Mortar prisms of the size 40×40×160 mm were produced for measurement of flexural and compressive strengths at different curing ages of 3, 7, 28, 60 and 90 days. First, according to ASTM C348-14 [22], each 40×40×160 mm prism was used for flexural strength measurement. Then, each of the two halves obtained from flexural strength measurement were used for compressive strength measurement in accordance with ASTM C109-16 [23]. The flexural and compressive strength were measured using a uniaxial digital hydraulic machine (SCL brand) with a capacity of 300 KN and an accuracy of ± 1%, controlled at a loading rate of 75 KN/min. For each measurement, two prisms were used. Therefore, flexural and compressive strength results are average of two and four measurements, respectively.

### *2.2.3. ITZ Microstructure*

28-day cured mortars were used for ITZ microstructural studies. For this reason, small pieces were cut from mortar prisms and dried at 60 ˚C for 72 h. The dried specimens were then coated with carbon after impregnation with epoxy and polishing. The ITZ microstructure was studied using a TESCAN VEGA II SEM operating at 30 kV and backscattered electron imaging (BSE) mode.

### *2.2.4. Chloride Penetration Depth*

28-days cured 40×40×160 mm mortar prisms were used for measurement of chloride penetration depth. For this reason, mortar prisms were cut from middle into two halves of equal sizes of 40×40×80 mm. Then all the faces were isolated with a bitumen layer except the 40×40 mm cut cross-section that was left prone to chloride penetration. The prepared specimens were then immersed in a 15 wt.% sodium chloride solution at a temperature controlled in the range 23.0 ± 2.0 ˚C. After 14 and 28 days of immersion, the specimens were removed and cut longitudinally into two halves of equal dimensions of 20×40×80 mm. To measure the chloride penetration depth, a solution of $AgNO_3$ with concentration of 0.1 mol/liter was lightly sprayed onto cut surfaces. The chemical reaction between penetrated chloride ion and silver nitrate resulted in the formation of a white precipitate that produced a color change in chloride penetrated areas. The chloride penetration depth was measured based on this color change [24].

### *2.2.5. Open-Pore Volume*

Two mortar specimens from each mortar (NM and RAM) with dimensions 100×100×100 mm were prepared and cured for open-pore volume measurements. The open-pore volume of the 28-day cured mortar specimens were measured according to with ASTM C642 [25]. For this, the specimens' dry weights (A) were firstly measured after drying them in an oven at 100 ˚C. Then, after submerging in water at 21 ˚C for enough time and boiling in water for 5 h, the fully-saturated weights (C) of the specimens were measured. Finally, the immersion weights (D) of the specimens were measured by suspending them in water. The open-pore volume of the mortar specimens was then determined using the following equation:



[ DOI: 10.22068/ijmse.18.1.5 ]

$$(\%)\ \text{open pore volume} = 100 \times \frac{C - A}{C - D} \qquad (1)$$

## 3. RESULTS AND DISCUSSION

### 3.1. Workability and Setting Time

Table 4 displays the results achieved from workability and setting time measurements. As seen, replacing natural quartz sand with PC clinker at the constant water-to-cement ratio of 0.545 poses negative effects on workability and setting time. It reduces workability by about 6% in terms of spread diameter. Setting time also displays a significant decrease of about 14% by this replacement. PC-clinker is known as a relatively porous material. Felekoğlu et al [26] performing porosity measurements on industrial PC clinkers reported total average porosities ranging from 20% to about 28%. In addition, PC clinker is a chemically reactive material and hydration reactions of clinker phases at its surface and during the early stages of material mixing consumes part of the mixing water. The significant water adsorption tendency of clinker both in the form of physisorption by its porous microstructure and in the form of chemisorption by its chemical reactivity is therefore responsible for significant reductions in both workability and setting time of RAM compared to NM.

### 3.2. Compressive and Flexural Strengths

The results of compressive and flexural strengths measurements at curing ages of 3, 7, 28, 60 and 90 days are shown in Figs. 1 and 2, respectively. According to these two figures, compressive and flexural strengths are significantly increased by quartz sand replacement with PC clinker. Compressive strength indicates a relatively large increment at early ages. The increment in 3-day and 7-day compressive strengths are approximately 44% and 65%, respectively. At later ages, however, the percentage of increase in compressive strength decreases and reaches to an almost constant value of 20% at 60 and 90 days. The increment in flexural strength, however, is lower and almost constant at about 14% at different curing ages. The significant increases in both compressive and flexural strengths in the RAM compared to NM are due to the ITZ microstructural improvements brought about by superficial hydration reactions of PC clinker. These microstructural improvements are more significant at early ages due to relatively fast superficial hydration reaction of PC clinker. At later ages, however, the surface of quartz sand in RAM undergoes a slow partial pozzolanic reaction [27] resulting in limited improvement in ITZ microstructure and reducing the amount of increment.

**Table 4.** Workability and setting time of normal and reactive-aggregate mortars.

| Mortar type | Spread diameter (mm) | Setting time (min) |
|---|---|---|
| NM | 112.23 | 62.78 |
| RAM | 105.88 | 54.00 |

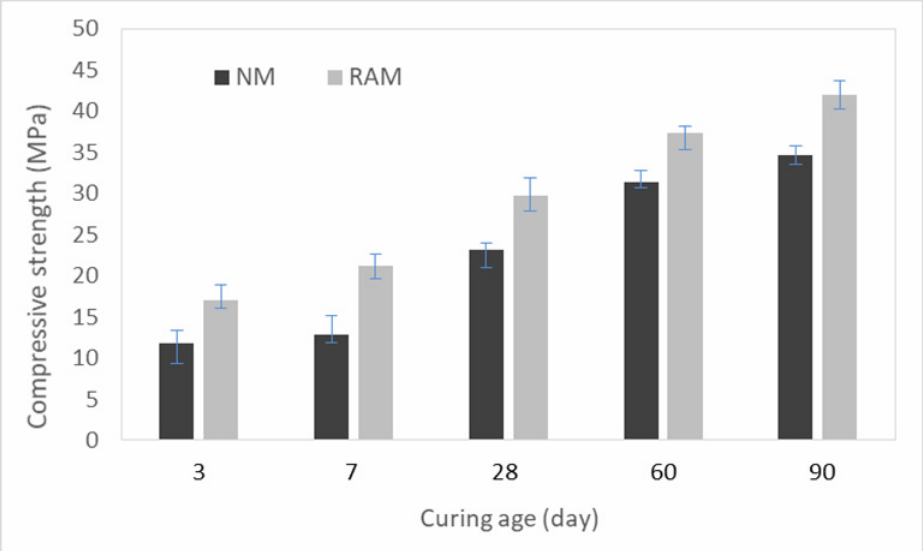


**Fig. 1.** Compressive strength of NM and RAM at different curing ages.



[ DOI: 10.22068/ijmse.18.1.5 ]

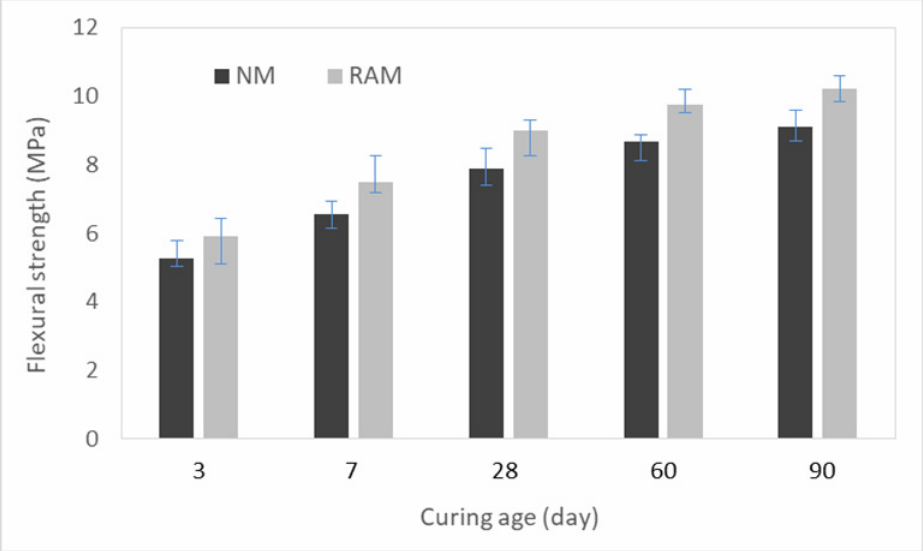


**Fig. 2.** Flexural strength of NM and RAM at different curing ages.

### 3.3. ITZ Microstructure

Investigations by BSE mode of SEM confirmed huge microstructural improvements in ITZ of RAM compared to NM. Fig. 3 represents typical SEM micrographs prepared from polished cut surfaces of NM and RAM. In the case of NM, as seen the cement paste matrix and the quartz sand particles are clearly distinguishable from their bright and dark gray colors, respectively. The porosity of the matrix and ITZ is also clearly distinguishable from its black color. In RAM image, however, the cement paste matrix is darker than PC clinker particles. As seen, in NM both cement paste matrix and ITZ represented relatively highly porous microstructures, whereas in RAM the porosity of ITZ microstructure was greatly reduced and a very good bonding between cement matrix and PC clinker was produced. These significant microstructural improvements in ITZ are due to superficial hydration reactions of clinker that produce enough binding compounds to effectively densify the ITZ and to produce a good bonding between the cement matrix and the PC clinkers. This ITZ microstructure improvement technique seems to be much more effective than other introduced techniques [1-11]. An accurate comparison, however, requires comprehensive comparative experimental data.

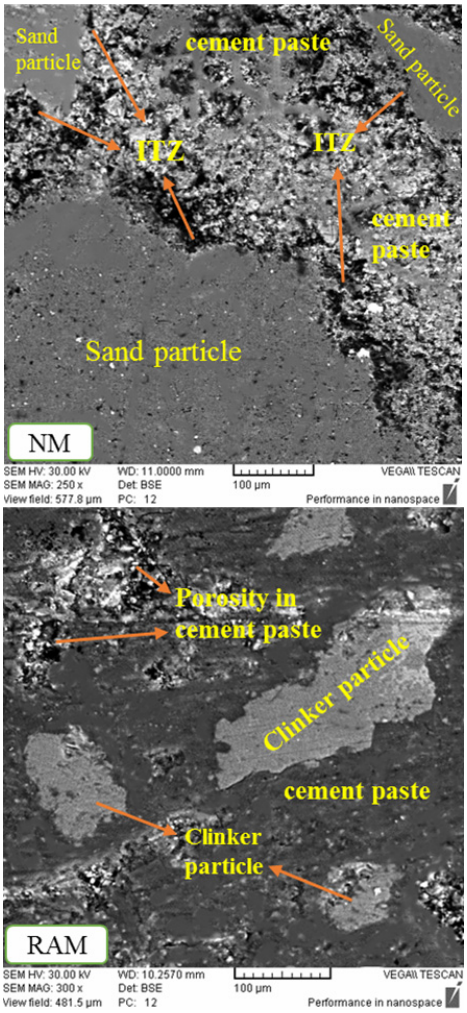


**Fig. 3.** SEM micrographs prepared from microstructures of NM and RAM



[ DOI: 10.22068/ijmse.18.1.5 ]

### 3.4. Chloride Penetration Depth

The results of chloride penetration depth measurements in NM and RAM after 14 and 28 days of immersion in 15 wt.% sodium chloride solution are presented in Table 5. These results show that replacement of quartz sand with PC clinker in RAM reduced the chloride penetration depths at 14 and 28 days by about 33% and 26%, respectively. These significant reductions in chloride penetration depth are in agreement with the other results and observations and confirm the ITZ microstructural improvements in RAM brought about by PC clinker.

**Table 5.** Chloride penetration depth in NM and RAM.

| Mortar type | Penetration (mm) | |
|---|---|---|
| | 14 days | 28 days |
| NM | 24 | 27 |
| RAM | 16 | 20 |

As seen, replacement of natural quartz sand with PC clinker in NM not only enhances compressive and flexural strengths of the mortar significantly, but also reduces its permeability considerably. Reduced permeability against chloride ion, however, cannot be considered as a proof for general long term durability of RAM compared to NM. The hydraulic property and chemical reactivity of anhydrous phases inside PC clinker particles may impose different effects on long term performance of this new mortar in different aggressive media. On the other hand, one positive potential effect of using PC clinker as a reactive aggregate could be a self-healing property in RAM. Late hydration of anhydrous clinker phases can result in the formation of enough calcium silicate hydrates that might effectively infill the damaging cracks caused by external disintegrating stresses. RAM, therefore, is a new material that requires extensive research activities for its properties including long term durability to be understood.

### 3.5. Open Pore Volume

The results of open-pore volume test of NM and RAM specimens after 28 days of curing are shown in Table 6. As seen, replacement of quartz sand with PC clinker resulted in about 21.7% reduction in total open-pore volume due to ITZ microstructural improvements. This reduction is in agreement with improvements observed in mechanical properties and chloride penetration depth and confirms the ITZ microstructural refinement due to replacement of sand with fine PC clinker.

**Table 6.** Open-pore volume of NM and RAM after 28 days of curing.

| Mortar type | Total open-pore volume (%) |
|---|---|
| NM | 8.85 |
| RAM | 6.93 |

## 4. CONCLUSION

Sand replacement with Portland cement clinker in mortar can effectively refine the microstructure of the interfacial transition zone and result in a relatively strong bonding between cement paste matrix and PC clinker surface used as aggregate. The new mortar referred to as Reactive Aggregate Mortar therefore exhibits superior engineering properties compared to the control normal mortar. Experimental results confirmed significant increase in both compressive and flexural strengths, as well as, significant reduction in ITZ porosity that resulted in noticeable decrease in both chlorine penetration depth and open-pore volume. The only drawback of this technique for ITZ microstructural improvement is the high price of clinker as well as high water absorption compared to natural quartz sand that limits the potential applications of the Reactive Aggregate Mortar.

## REFERENCES

1. J. Ollivier, J. Maso, B. Bourdette, “Interfacial transition zone in concrete”, Advanced Cement Based Materials, 1995, 2, 30-38.
2. J. Zheng, Q. Li, X. Zhou, “Thickness of interfacial transition zone and cement content profiles around aggregates”, Magazine of Concrete Research, 2005, 57(7), 397-406.
3. E. Garboczi, D. Bentz, “The Effect of the Interfacial Transition Zone on Concrete Properties: The Dilute Limit”, American Society of Civil Engineers, Proceedings of the Fourth Materials Conference, Washington DC, 1996.



[ DOI: 10.22068/ijmse.18.1.5 ]

4. K. L. Scrivener, A. Crumbie, P. Laugesen, "The Interfacial Transition Zone (ITZ) Between Cement Paste and Aggregate in Concrete", Interface Science, 2004, 12, 411-421.
5. G. Prokopski, J. Halbiniak, "Interfacial transition zone in cementitious materials", Cement and Concrete Research, 2000, 30, 579-583.
6. K. Li, P. Stroeven, M. Stroeven, L. Sluys, "A numerical investigation into the influence of the interfacial transition zone on the permeability of partially saturated cement paste between aggregate surfaces", Cement and Concrete Research, 2017, 102, 99-108.
7. M. Nili, A. Ehsani, "Investigating the effect of the cement paste and transition zone on strength development of concrete containing nanosilica and silica fume", Materials and Design, 2015, 75, 174-183.
8. M.D. Cohen, A. Goldman, W. Chen, "The role of silica fume in mortar: transition zone versus bulk paste modification", Cement and Concrete Research, 1997, 24, 95-98.
9. P. Duan, Z. Shui, W. Chen, C. Shen , "Effects of metakaolin, silica fume and slag on pore structure, interfacial transition zone and compressive strength of concrete", Construction and Building Materials, 2013, 44, 1-6.
10. S. Cheng, Z. Shui, T. Sun, R. Yu, G. Zhang, S. Ding, "Effects of fly ash, blast furnace slag and metakaolin on mechanical properties and durability of coral sand concrete", Applied Clay Science, 2017, 141, 111-117.
11. Z. He, C. Qian, S. Du, M. Huang, M. Xia, "Nanoindentation characteristics of cement paste and interfacial transition zone in mortar with rice husk ash", Journal of Wuhan University of Technology-Mater. Sci. Ed., 2017, 32, 417-421.
12. H. Chao-Lung, B. L. Anh-Tuan, C. Chun-Tsun, "Effect of rice husk ash on the strength and durability characteristics of concrete", Construction and Building Materials, 2011, 25, 3768-3772.
13. A. N. Givi, S. A. Rashid, F. N. A. Aziz, M. A. Mohd Salleh, "Assessment of the effects of rice husk ash particle size on strength, water permeabiity and workability of binary blended concrete", Construction and Building Materials, 2010, 24, 2145-2150.
14. X. Ping, J. J. Beaudoin, R. Brousseau, "Effect of aggregate size on transition zone properties at the Portland cement paste interface", Cement and Concrete Research, 1991, 21, 999-1005.
15. R. L. Berger, "Properties of concrete with cement clinker aggregate", Cement and Concrete research. 1974, 4, 99-112.
16. J. Shafaghat and A. Allahverdi, "Using PC clinker as aggregate-Enhancing concrete properties by improving ITZ microstructure", Magazine of Concrete Research. 2019, published on line. doi: 10.1680/jmacr.18.00134
17. ASTM C150-17, Standard specification for Portland cement, 2017, ASTM International, West Conshohocken, PA, USA.
18. ASTM C192-16, Standard Practice for making and curing concrete test specimens in the laboratory, 2016, ASTM International, West Conshohocken, PA, USA.
19. ASTM C230-14, Standard specification for flow table for use in tests of hydraulic cement, 2014, ASTM International, West Conshohocken, PA, USA.
20. ASTM C1437-15, Standard test method for flow of hydraulic cement mortar, 2015, ASTM International, West Conshohocken, PA, USA.
21. ASTM C807-13, Standard test method for time of setting of hydraulic cement mortar by modified Vicat needle, 2013, ASTM International, West Conshohocken, PA, USA.
22. ASTM C348-14, Standard test method for flexural strength of hydraulic-cement mortars, 2014, ASTM International, West Conshohocken, PA, USA.
23. ASTM C109-16, Standard test method for compressive strength of hydraulic cement mortars using 2-in. or [50-mm] cube specimens, 2016, ASTM International, West Conshohocken, PA, USA.
24. F. He, C. Shi, Q. Yuan, Ch. Chen, K. Zhengt, "$AgNO_3$-based colorimetric methods for measurement of chloride penetration in concrete", Construction and Building Materials, 2012, 26, 1-8.
25. ASTM C642, Standard test method for specific gravity, absorption and voids in hardened concrete1990, ASTM International, West Conshohocken, PA, USA.



[ DOI: 10.22068/ijmse.18.1.5 ]

26. B. Felekoğlu, K. Tosun, B. Baradan, A. Altun, "Effects of porosity and related interstitial phase morphology difference on the grindability of clinkers", Materials and Structures, 2010, 43, 179-193.
27. S. Agarwal, "Pozzolanic activity of various siliceous materials", Cement and Concrete Research, 2006, 36, 1735-1739.



[ DOI: 10.22068/ijmse.18.1.5 ]